Muscle Artifacts in Single Trial EEG Data Distinguish Patients with Parkinson's Disease from Healthy Individuals

Jonathan Weyhenmeyer[1,2], Manuel E. Hernandez[3], Claudia Lainscsek[1,3], Terrence J. Sejnowski[1,3], and Howard Poizner[3,4]

***Abstract*— Parkinson's disease (PD) is known to lead to marked alterations in cortical-basal ganglia activity that may be amenable to serve as a biomarker for PD diagnosis. Using non-linear delay differential equations (DDE) for classification of PD patients on and off dopaminergic therapy (PD-on, PD-off, respectively) from healthy age-matched controls (CO), we show that 1 second of quasi-resting state clean and raw electroencephalogram (EEG) data can be used to classify CO from PD-on/off based on the area under the receiver operating characteristic curve (AROC). Raw EEG is shown to classify more robustly (AROC=0.59-0.86) than clean EEG data (AROC=0.57-0.72). Decomposition of the raw data into stereotypical and non-stereotypical artifacts provides evidence that increased classification of raw EEG time series originates from muscle artifacts. Thus, non-linear feature extraction and classification of raw EEG data in a low dimensional feature space is a potential biomarker for Parkinson's disease.**

I. INTRODUCTION

Parkinson's disease (PD) is the second most common chronic neurodegenerative disorder of the central nervous system affecting approximately 1% of the population over 60 years of age [1]. Since the initial description of PD, it has been predominantly diagnosed and treated as a disease of the motor system [2]. More recent work has shown that PD is present pathologically throughout the nervous system [3]. Indeed, clinically discernible motor symptoms may be a late manifestation of PD [4]. As such, it is imperative that we begin to look for biomarkers of PD to provide additional tools to aid clinicians in early and correct diagnoses.

Non-linear time series analysis techniques have been applied to neurological diseases such as epilepsy [5] and PD [6], [7]. Previously, our group has shown that non-linear delay differential equations (DDEs) are able to classify the difference between healthy control (CO), Parkinson-off (PD-off) and Parkinson-on (PD-on) medication using clean clustered EEG data [8], [9]. This classification strongly correlates with an individual's present state of pathology as measured by clinical UPDRS measurements. The ability to distinguish PD subjects from healthy control subjects based solely on single electrode raw EEG data is a necessary step towards clinical implementation as it is not tractable for a clinician to both acquire and process EEG data prior to implementing a classification algorithm. In the following study we compare DDE feature extraction and classification of clean and raw EEG data in order to differentiate PD and healthy subjects.

This work was supported by the Howard Hughes Medical Institute, NSF grant #SMA-1041755, NSF ENG-1137279 (EFRI M3C), and ONR MURI Award No.: N00014-10-1-0072.

[1] Howard Hughes Medical Institute, Computational Neurobiology Laboratory, The Salk Institute for Biological Studies, La Jolla, CA, USA

[2] Indiana University School of Medicine, Indianapolis, IN, USA

[3] Institute for Neural Computation, University of California at San Diego, La Jolla, CA, USA

[4]Graduate Program in Neurosciences, University of California, San Diego, La Jolla, CA, USA

II. METHODS

A. Non-linear classification

According to Cover's theorem, time-series that are linearly inseparable can be put through a non-linear transformation kernel and projected into a non-linear space whereby the the time series become linearly separable [10], [11]. If the non-linear transformation is assumed to provide linear separability, it is then possible to train a weight matrix W using singular value decomposition (SVD) that maximally separates the data such that classification is performed by hyper-planing the feature space (Fig. 1). The linear separation prior to classification is ideal because it allows for the use of SVD and avoids the complexity and computational cost associated with non-linear separation algorithms, e.g. support vector machines and probabilistic neural networks.

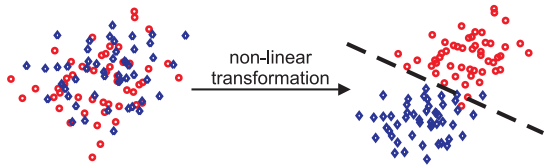

Fig. 1. Diagram of Cover's theorem. Two classes of data, red circles and blue diamonds, are shown to be linearly inseparable prior to a non-linear transformation (right). After the non-linear transformation (left) a hyperplane (dashed line) can be applied that maximally separates the data into two distinct classes.

B. Delay Differential Equations

A delay differential equation (DDE) is a functional embedding technique that transforms a time series into a multi-dimensional geometrical object. The DDE should be considered a generic non-uniform embedding of a signal $x(t)$ that relates the derivative of a signal $\dot{x}(t)$ to a function of the signal itself and/or its delayed versions x_τ where $x_\tau = x(t-\tau)$. A general DDE takes the form

$$\dot{x} = f(x, x_{\tau_1}, x_{\tau_2}, \ldots x_{\tau_n}) \quad (1)$$

with l monomials, n delays, and order m non-linearity. The DDE is generic because it is the combination of two embedding techniques, the derivative and delay embedding. The DDE is non-uniform because the delays are not required to be multiples of each other. Even though DDE analysis is

978-1-4244-7929-0/14/$26.00 ©2014 IEEE

done in the time domain and not the spectral domain there are relations between frequencies and time delays. Delays found in linear DDE terms are related to specific frequencies found within the signal and delays found in higher order terms, x_τ^m, are associated with higher order couplings between frequencies [12]. The monomial coefficients $a_1, a_2, ..., a_n$ are related to all of the frequencies in the signal. The error ρ is the deviation of the model output $f(x_{\tau_i})$ from the signal derivative $\dot{x}$. ρ is calculated with mean-squared error estimation $\rho = \sqrt{\sum(\dot{x} - f(x_{\tau_i}))^2}$. ρ is minimized for each model-delay combination through numerical optimization of the coefficients using least squares SVD [13]. The coefficients a_i and ρ are considered non-linear features on which a linear classification can be performed for two classes such that,

$$\mathbf{A}_i \cdot \mathbf{W}_i = \mathbf{S}_i = \begin{cases} 0 & i \in Class\ 1 \\ 1 & i \in Class\ 2 \end{cases} \tag{2}$$

where $\mathbf{A}_i$ is a DDE-feature matrix for subject i and W is a weight matrix that maps the subjects features to a 1-dimensional space either above or below a hyperplane [8].

The analysis in this paper was limited to two delays and monomials up to cubic nonlinearities,

$$\begin{aligned} \dot{x} &= f(x_{\tau_1}, x_{\tau_2}) = \\ &= a_1 x_{\tau_1} + a_2 x_{\tau_2} + a_3 x_{\tau_1}^2 + a_4 x_{\tau_1} x_{\tau_2} + a_5 x_{\tau_2}^2 + \\ &\quad a_6 x_{\tau_1}^3 + a_7 x_{\tau_1}^2 x_{\tau_2} + a_8 x_{\tau_1} x_{\tau_2}^2 + a_9 x_{\tau_2}^3 . \end{aligned} \tag{3}$$

The time delay τ_n in each term of the DDE ranged from 1-50 time-steps δt where $1\delta t = \frac{1}{f_s}$ and $f_s = 512$ Hz is the sampling rate. The models ranged from 1 to 3 monomial terms, thus 69 models were included in the analysis. Model-delay pairs were used to generate a feature space for all trials resulting in an error coefficient feature set for each trial.

C. Training and Validation

Training and testing of model-delay pairs and associated weight matrices is performed by splitting the data into a training set, 2/3 of data, and a validation set 1/3 of data. The training data is then randomly subsampled into train, 2/3 of subjects, and test sets, 1/3 of subjects (Fig. 2). The

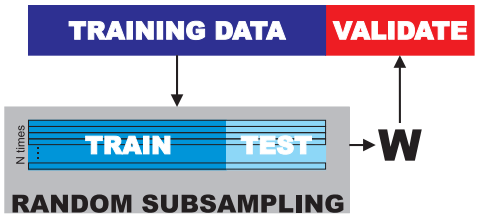

Fig. 2. Training and validation of a weight matrix W trained on non-linear DDE features from all trials for subjects in the binary classifier. The weight matrix is trained with repeated random subsampling and then validated on the validation data set.

random subsampling of the training data into training and testing sets is repeated 84 times for each of the model-delay combinations and best performing weight matrix W is generated by averaging across all 84 Ws for each model-delay pair. The W is then applied to the validation set and the area under the receiver operating characteristic (AROC) defines how well the classifier performed. This process is repeated for each electrode for each binary classifier. Prior to training and testing, the number of trials across all three classes was equalized to avoid biasing the classifiers. For additional explanation of this procedure see [8], [14].

III. Materials and Methods

A. Hardware

Electroencephalographic (EEG) data were collected using a 70-channel active electrode EEG system (Biosemi Inc. ActiveTwo, Amsterdam, Netherlands) consisting of a cap plus four EOG electrodes, temporal to both eyes and above and below the right eye, two EMG electrodes on the trapezius and right and left sternocleidomastoids, and two reference electrodes on the left and right mastoids. Data were recorded with a 512 Hz sampling rate, and referenced to the averaged mastoid electrodes. Head position relative to the EEG sensors was determined with an electromagnetic motion tracking system (Polhemus, FASTRAK, Colchester, VT, USA).

B. Participants

Nine PD patients on and off dopaminergic therapy (6 females, mean ± SD age: 62.8 ± 8.5 years) and ten age-matched healthy older adults participated in this study (4 females, mean ± SD age: 66.1 ± 9.3 years). No participant had any neurological or psychiatric disease in addition to PD for the the PD participants. All participants were right-hand dominant with normal or corrected to normal vision. All participants signed the informed consent document approved by the human subjects Institutional Review Board of the University of California, San Diego.

C. Protocol

Participants reached for and grasped a virtual rectangular object (3.5 x 8.5 x 6 cm) with haptic feedback provided to the thumb and index finger by two 3-degree of freedom haptic robotic devices (Phantom Premium 1.0, Geomagic, Wilmington, MA, USA) at the sound of a tone, as described previously [15]. Overall, a maximum of 360 (10 blocks of 36 trials) trials were performed by each participant, with rest provided between blocks to limit fatigue. In this study, we considered EEG data from one second before the tone stimulus to the tone stimulus.

D. Data Processing and Analysis

In this study, we analyzed both raw and clean back-projected EEG data. To get clean data, raw EEG data were first imported into EEGLAB using MATLAB (The MathWorks, Natick, MA, USA) for processing [16]. Data were then high-pass filtered at 1 Hz to remove drift and low-pass filtered at 55 Hz to remove line noise. EEG artifacts associated with eye and other muscle movement were removed using independent component analysis (ICA) [17]. Based on the topography, spectra, and trial-to-trial characteristics of ICA components, non-artifactual components were selected and used to generate clean back-projected EEG data while

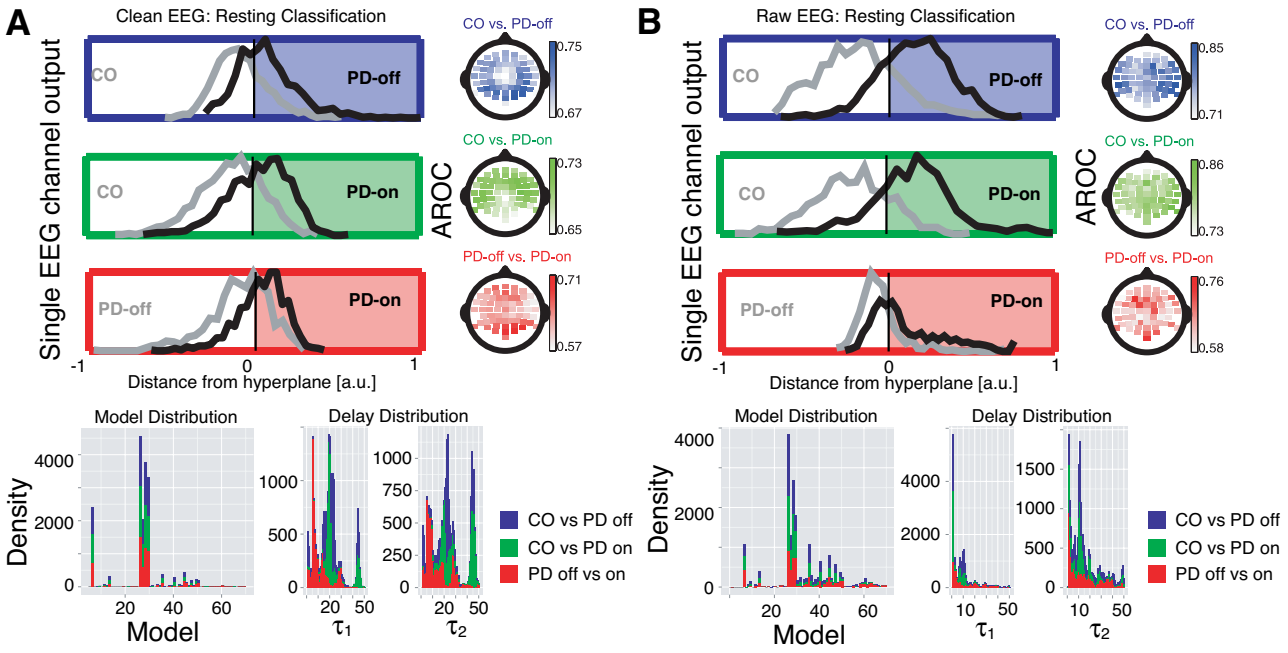

Fig. 3. A) Classification performance, based on the area under the ROC curve (AROC), of the three classifiers (Control vs. PD off [blue], Control vs. PD on [green], and PD off vs. on [red]) on clean EEG data presented as max-min normalized topographical representations on the right and density plots for the distance from the hyperplane for each classifier is shown on the left, and characteristic model and delay distribution in a 100 model-delay combinations with the best classification performance below. B) Similar classification performance, model and delay distributions in raw EEG data.

the remaining components were used to generate artifactual IC back-projected EEG data. Further breakdown of the artifactual IC group was performed by manually separating ICs into stereotypical muscle, electrode, eye, and unsure artifact classes based on topography, spectra, and trial-to-trial characteristics.

IV. RESULTS

Overall, for distinguishing PD patients off medication (PD-off) from healthy controls (CO), classification performance (AROC) on individual 1-s samples of clean EEG data ranged from 0.67 to 0.75 across individual electrodes using the top model-delay combination (Fig. 3 A). Classification performance for distinguishing PD patients on medication (PD-on) from controls ranged from 0.65 to 0.73 and for distinguishing PD patients on and off medication performance ranged from 0.57 to 0.72. Surprisingly, using raw, unprocessed, EEG data resulted in modest classification performance improvements in CO versus PD-off ($AROC = 0.71 - 0.85$), CO versus PD-on ($AROC = 0.74 - 0.86$) and PD-off versus PD-on ($AROC = 0.59 - 0.74$). To evaluate the effect of electrode location and classifier on classification we used an analysis of variance on the AROC of the top 100 model-delay pairs while controlling for the model-delay pair. A strong electrode location, classifier, and electrode by classifier interaction effect was observed for both raw and clean EEG data ($p < .00001$), using R version 3.0.1[18].

For both clean and raw EEG data, similar DDE models were most frequently selected across all three classifiers with higher order quadratic and cubic terms most commonly chosen. However, time delays were sensitive to both classifier and type of data, with smaller time delays ($\approx 10\delta t$ vs. $\approx 20\delta t$) most often selected for raw data.

In order to better understand how improved classification performance was achieved on the raw EEG data, we examined the changes in dynamics observed in back-projected muscle ICs, eye ICs, electrode ICs, and other unclassified ICs. Classification was initially performed on all artifactual ICs, e.g. combination of muscle, eye, electrode and unsure ICs, yielding a strong performance ($AROC = 0.76 - .92$) when comparing CO to PD-off and PD-on. The performance was significantly worse when classifying PD-off against PD-on ($AROC = .64 - .77$) (Fig. 4). Further IC decomposition

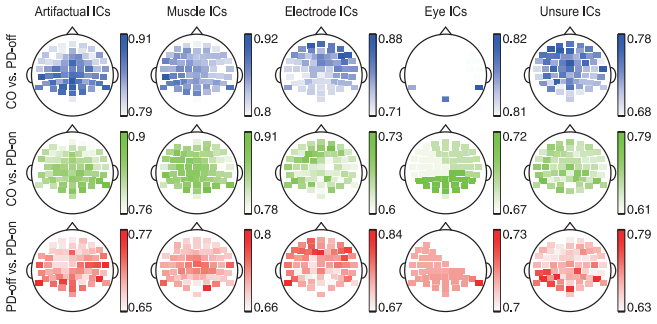

Fig. 4. Classification performance across the backprojection of all artifactual, muscle, eye, electrode, and unsure ICs with the strongest classification performance seen in the back projected muscle ICs.

was performed by separating the artifactual ICs into the aforementioned classes. The muscle IC class displayed the best classification with similar classification for both CO versus PD-off ($AROC = .79 - .92$) and CO versus PD-on ($AROC = .76 - .90$) and followed a similar spatial pattern to the classification of the backprojection of all

artifactual ICs. Importantly, the ranking of performance, e.g. CO versus PD-off AROC is about equal to CO versus PD-on AROC and both classifiers perform significantly better than the PD-off versus PD-on classifier, is very similar to both raw data and the back projected artifactual ICs. Performance for the remaining IC classes was also quite good, however the spatial distribution of performance across electrodes was quite different from the artifactual ICs and the raw data classification. Additionally, the ranking of the classifiers for each of the artifact types differed dramatically for each of the remaining artifactual IC classes. The spatial classification of the back projected artifactual ICs was found to correlate most strongly with the classification of the back-projected muscle ICs for CO versus PD-off ($R = .46, p < .001$), CO versus PD-on ($R = .55, p < .00001$) and PD-off versus PD-on ($R = .25, p < .05$). No correlations between the raw data classification and the back projected IC groups reached significance.

V. Discussion and conclusion

In the present study, we have shown the classification of CO and PD-on/off subjects using non-linear DDE features obtained from single electrode, 1 second quasi-resting state clean and raw EEG data. Raw EEG data was considerably better at classifying the difference between PD-on/off and control than clean EEG data. In comparison to clean EEG data, the raw EEG classification is much more spatially coarse, with improved classification at the edges of the EEG cap, indicating that the improved classification is likely dependent upon artifacts. Indeed, further analysis provided evidence that muscle artifacts were a large contributor to the improved classification based on artifactual IC classification, classifier ranking and spatial correlations. Importantly, muscle artifacts would be expected to be a significant contributor to the performance of the three classifiers ($AROC = 0.67 - 0.92$) because PD patients often experience rigidity and dopaminergic therapy is thought to partially alleviate these symptoms.

While it would be ideal to identify true differences in cortical processing between PD-on/off and controls that scaled with pathology, the improved classification on raw EEG data, predominantly independent of electrode placement (Fig. 3 B) is much easier to utilize in a clinical or physical therapy setting. Indeed, raw EEG data by its definition does not require any artifact rejection, filtering, or manually performed ICA cleaning. Such a system is immensely useful to a non-technical operator because it acts as a black box that a user would need to know very little about. Furthermore, the finding that the classification between all three groups based on raw EEG data could be performed with a single DDE model ($\dot{x} = x_{\tau_1} + x_{\tau_2} + x_{\tau_1}^2$) and set of delay pairs e.g. $10\delta t$ and $20\delta t$ (Fig. 3 B), indicates that the non-linear DDE classification scheme is identifying stereotyped differences that hold at the class level, e.g. healthy control or Parkinsonian.

This study was performed on a limited set of Parkinsonian and healthy control subjects during the quasi-resting state of a movement task. In order to understand how the algorithm would scale to resting data in the general population, a much larger sample size would need to be tested on true resting state data. However, the present analysis provides an initial proof of concept for a raw EEG data classification tool that is able to discriminate between healthy control and Parkinsonian patients both on and off medication.

Acknowledgment

We would like to thank Sofia Campos, Luke Miller, Jamie Lukos, Markus Plank, and Joseph Snider for their help with equipment setup and data collection, as well as all the volunteers who participated in this study.

References

[1] L. M. de Lau and M. M. Breteler, "Epidemiology of parkinson's disease," *The Lancet Neurology*, vol. 5, no. 6, pp. 525 – 535, 2006.

[2] J. Jankovic, "Parkinsons disease: clinical features and diagnosis," *J Neurol Neurosurg Psychiatry*, vol. 79, no. 4, pp. 368–376, 2008.

[3] H. Braak, K. D. Tredici, U. Rb, R. A. de Vos, E. N. J. Steur, and E. Braak, "Staging of brain pathology related to sporadic parkinsons disease," *Neurobiology of Aging*, vol. 24, no. 2, pp. 197 – 211, 2003.

[4] A. E. Lang and J. A. Obeso, "Challenges in parkinson's disease: restoration of the nigrostriatal dopamine system is not enough," *The Lancet Neurology*, vol. 3, no. 5, pp. 309 – 316, 2004.

[5] K. Lehnertz, "Epilepsy and nonlinear dynamics," *Journal of Biological Physics*, vol. 34, pp. 253–266, 2008.

[6] L. Pezard, R. Jech, and E. Ruzicka, "Investigation of non-linear properties of multichannel eeg in the early stages of parkinson's disease," *Clinical Neurophysiology*, vol. 112, pp. 38–45, 2001.

[7] V. Muller, W. Lutzenberger, F. Pulvermuller, B. Mohr, and N. Birbaumer, "Investigation of brain dynamics in parkinson's disease by methods derived from non-linear dynamics," *Exp Brain Research*, vol. 137, pp. 103–110, 2001.

[8] C. Lainscsek, J. Weyhenmeyer, M. E. Hernandez, H. Poizner, and T. J. Sejnowski, "Non-linear dynamical classification of short time series of the rssler system in high noise regimes," *Frontiers in Neurology*, vol. 4, no. 182, 2013.

[9] C. Lainscsek, M. E. Hernandez, J. Weyhenmeyer, T. J. Sejnowski, and H. Poizner, "Non-linear dynamical analysis of eeg time series distinguishes patients with parkinsons disease from healthy individuals," *Frontiers in Neurology*, vol. 4, no. 200, 2013.

[10] T. Cover, "Geometrical and statistical properties of systems of linear inequalities with applications in pattern recognition," *Electronic Computers, IEEE Transactions on*, vol. EC-14, no. 3, pp. 326–334, June 1965.

[11] D. Garrett, D. Peterson, C. Anderson, and M. Thaut, "Comparison of linear, nonlinear, and feature selection methods for eeg signal classification," *Neural Systems and Rehabilitation Engineering, IEEE Transactions on*, vol. 11, no. 2, pp. 141–144, June 2003.

[12] C. Lainscsek and T. Sejnowski, "Electrocardiogram classification using delay differential equations," *Chaos*, vol. 23(2), p. 023132, 2013.

[13] W. Press, B. Flannery, S. Teukolsky, and W. Vetterling, *Numerical Recipes in C*. Cambridge University Press, 1990.

[14] R. Kohavi, "A study of cross-validation and bootstrap for accuracy estimation and model selection," in *Proceedings of the 14th international joint conference on Artificial intelligence - Volume 2*, ser. IJCAI'95. Morgan Kaufmann Publishers Inc., 1995, pp. 1137–1143.

[15] J. Lukos, J. Snider, M. Hernandez, E. Tunik, S. Hillyard, and H. Poizner, "Parkinson's disease patients show impaired corrective grasp control and eye-hand coupling when reaching to grasp virtual objects," *Neuroscience*, p. doi:10.1016/j.neuroscience.2013.09.026, 2013.

[16] A. Delorme and S. Makeig, "Eeglab: an open source toolbox for analysis of single-trial eeg dynamics including independent component analysis," *J Neurosci Methods*, vol. 134, no. 1, pp. 9–21, 2004.

[17] T. Jung, S. Makeig, C. Humphries, T. Lee, M. McKeown, V. Iragui, and T. Sejnowski, "Removing electroencephalographic artifacts by blind source separation," *Psychophysiology*, vol. 37, no. 2, pp. 163–78, 2000.

[18] R Core Team, *R: A Language and Environment for Statistical Computing*, R Foundation for Statistical Computing, Vienna, Austria, 2013. [Online]. Available: http://www.R-project.org/